Journal of Pharmacological Sciences 146 (2021) 58–64

Contents lists available at ScienceDirect

Journal of Pharmacological Sciences

journal homepage: www.elsevier.com/locate/jphs

Full Paper

Differentially regulated pools of aquaporin-4 (AQP4) proteins in the cerebral cortex revealed by biochemical fractionation analyses

Julia Ramadhanti [a, e], Tomoko Yamada [a], Masato Yasui [a, d], Mutsuo Nuriya [a, b, c, d, *]

[a] Department of Pharmacology School of Medicine, Keio University, 35 Shinanomachi, Shinjuku-ku, Tokyo, 160-8582, Japan
[b] Graduate School of Environment and Information Sciences, Yokohama National University, Kanagawa, 240-8501, Japan
[c] Precursory Research for Embryonic Science and Technology (PRESTO), Japan Science and Technology Agency (JST), Kawaguchi, Saitama, 332-0012, Japan
[d] Keio Advanced Research Center for Water Biology and Medicine, Keio University, 2-15-45 Mita, Minato-ku, Tokyo, 108-8345, Japan
[e] Department of Biomedical Science, Medical Faculty, Universitas Padjadjaran, Jalan Professor Eijkman no.38, Bandung, 40161, Indonesia

ARTICLE INFO

Article history:
Received 7 February 2021
Received in revised form
5 March 2021
Accepted 9 March 2021
Available online 17 March 2021

Keywords:
Aquaporin-4
AQP4 isoforms
Detergent fractionation
Oxygen-glucose deprivation
Detergent-resistant membrane

ABSTRACT

Aquaporin-4 (AQP4) is a predominant water channel in the central nervous system. It regulates water movement in the brain and has been suggested to play critical roles in various pathological conditions. However, the molecular mechanisms underlying its regulation are not yet well understood. In this study, we biochemically characterized AQP4 in the brain using acute cortical brain slices prepared from mice. Using biochemical fractionation, we found that AQP4 is enriched in the detergent-resistant membrane (DRM) fraction that is not soluble in 1% Triton X-100. In contrast, β-dystroglycan and syntrophin, which are part of the dystrophin complex in the brain, primarily reside in the non-DRM fraction. DRM enrichment of AQP4 is insensitive to cholesterol depletion, suggesting that it is not tightly associated with lipid rafts. Furthermore, AQP4 in the DRM fraction is more enriched in the M23 isoform than in the non-DRM fraction. Finally, by employing oxygen-glucose deprivation (OGD), an *in vitro* model of ischemia, we examined the molecular changes of AQP4. Under OGD conditions, a reduction in AQP4 in the DRM fraction was observed before the total AQP4 protein level dropped. Our data therefore highlight the characteristics of two pools of AQP4 that are distinctly regulated under ischemic conditions.

1. Introduction

Aquaporins are integral membrane proteins that facilitate water movement across the plasma membrane. There are thirteen known types in mammals, and only a handful of them are well studied.[1,2] One type of this membrane channel is aquaporin-4 (AQP4), which predominantly resides in the central nervous system. Its localization is polarized at the endfeet of astrocytes and regulates the movement of water in the brain.[2–4] An increase in brain water content, or brain edema, is the result of progression in an injury to the brain, such as trauma,[5] ischemia,[6] or tumors.[7] AQP4, a primary water channel in the brain, plays an important role in the accumulation of water in these pathophysiological conditions. It has been shown that AQP4 knockout mice have lesser brain edema and show better neurological outcomes than wild-type mice in a water intoxication model.[8] AQP4 is also involved in the autoimmune disease neuromyelitis optica.[9]

AQP4 has two major isoforms, M1 and M23. These two isoforms have 22 amino acid differences in the cytoplasmic N-terminal of the protein.[10] In the plasma membrane, AQP4 M1 isoforms tend to form singular tetramers, but M23 isoforms are more likely to form large arrays known as orthogonal array particles (OAPs). The ratio between M1 and M23 determines the size of these arrays.[11] In one study, Chinese hamster ovary (CHO) cells expressing both M1 and M23 had a more intermediate size of arrays compared to cells expressing only M1 or M23. The AQP4 M1 isoform has been shown to be the limiting factor for array size. Several hypotheses have been proposed to regulate the arrangement of these two isoforms in the plasma membrane. The large arrays are more stable in the plasma membrane relative to singular tetramers, as shown in an experiment related to the migration of astrocyte lamellipodia.[12] In a study of neuromyelitis optica, it was also revealed that large arrays are

* Corresponding author. Department of Pharmacology School of Medicine, Keio University, 35 Shinanomachi, Shinjuku-ku, Tokyo, 160-8582, Japan. Fax: +81 3 3359 8889.
E-mail address: mnuriya@z2.keio.jp (M. Nuriya).
Peer review under responsibility of Japanese Pharmacological Society.

https://doi.org/10.1016/j.jphs.2021.03.003

more resistant to endocytosis than singular tetramers.[13] Using quantum dot tracking, AQP4 single tetramers were found to move more freely compared to large arrays.[14] However, the significance of these forms in the plasma membrane is still not clear.

Fractionation based on detergent solubility is one method used to analyze proteins in the plasma membrane. The detergent-resistant membrane (DRM) fraction has been associated with lipid rafts, a microdomain in the plasma membrane rich with cholesterol and sphingolipid that is involved in membrane trafficking, membrane signaling, or influencing membrane fluidity.[15,16] Only a few studies have investigated the targeting of AQP4 in the DRM fraction. Using primary cultures, Noel et al.[17] mentioned that AQP4 may be located in the raft microdomain and participate in the regulation of AQP4 channels. On the other hand, Nicchia et al.[18] did not find the AQP4 pool in muscle to be co-purified with caveolin, a membrane marker of lipid rafts, instead suggesting that OAPs may be changed under pathophysiological conditions. In order to investigate the relationship between AQP4 and its membrane domain in the physiological context, we utilized acute brain slices and characterized the protein in the DRM and non-DRM fractions using detergent fractionation. We also investigated the distribution changes of both isoforms using an *in vitro* model of ischemia as a means of observing potential changes under pathological conditions. Our data show the need for fractionation in order to obtain a detailed characterization of AQP4 under physiological and pathological conditions.

2. Materials and methods

2.1. Brain slice preparation

Animal experiments were performed according to the Guidelines for the Care and Use of Laboratory Animals of Keio University School of Medicine. The method used for preparing brain slices was essentially the same as the one described by Gondo et al.[19] The mice were anesthetized using isoflurane, and after decapitation, the brain was placed in ice-cold cutting solution (222 mM sucrose, 27 mM $NaHCO_3$, 2.6 mM KCl, 1.5 mM NaH_2PO_4, 0.5 mM $CaCl_2$, and 7 mM $MgCl_2$) bubbled with 95% O_2/5% CO_2 at pH 7.4. The cerebellum and anterior part of the brain were cut and then mounted onto a Leica VT 1200 Microtome (Leica Microsystems, Wetzlar, Germany). A 300 μm slice was made using the microtome and subsequently immersed in a solution of artificial cerebrospinal fluid (ACSF) containing 126 mM NaCl, 3 mM KCl, 1.14 mM NaH_2PO_4, 26 mM $NaHCO_3$, 3 mM $CaCl_2$, 1 mM $MgCl_2$, and 10 mM dextrose pre-warmed to 37 °C and bubbled with 95% O_2/5% CO_2 at pH 7.4. The slices were incubated in this solution for 30 min before use.

Our investigation to determine the involvement of lipid rafts was performed by utilizing cholesterol depletion using methyl-β-cyclodextrin (MβCD). The brain slices were incubated in ACSF containing 2–8 mM MβCD or control solution for 60 min at 37 °C.[20] After this procedure, the slices were placed in ACSF to undergo the process of separating the two non-DRM and DRM fractions and were prepared for Western blotting as described in subsequent sections.

2.2. Oxygen-glucose deprivation (OGD)

After incubation in ACSF solution for 30 min at 37 °C, the slices were then placed in a 6-well plate with ACSF containing dextrose bubbled with 95% O_2/5% CO_2 for control or ACSF in which dextrose was replaced by sucrose bubbled with 95% N_2/5% CO_2 for OGD. The slices were incubated in these two solutions for 30 min at 37 °C. Then, they were processed for Western blotting.

2.3. Western blotting

The brain slices were rinsed in ice-cold 4-(2-hydroxyethyl)-1-piperazineethanesulfonic acid (HEPES) ACSF (125 mM NaCl, 5 mM KCl, 10 mM dextrose, 10 mM HEPES, 1 mM $MgCl_2$, and 2 mM $CaCl_2$ at pH 7.3) and homogenized in Triton buffer (1% Triton X-100 in phosphate-buffered saline) supplemented with a protease inhibitor cocktail (Roche Applied Science, Penzburg, Germany) and phosphatase inhibitor cocktail (Nacalai Tesque, Kyoto, Japan) at 4 °C for 30 min with gentle rotation. The lysate was then centrifuged at 20,000×*g* at 4 °C for 20 min. The supernatants comprised the non-DRM fraction and were collected and placed on ice. The pellet was then added to radioimmunoprecipitation assay (RIPA) buffer (1% Triton X-100, 0.1% sodium dodecyl sulfate, 0.5% deoxycholic acid, 50 mM Tris–HCl, 100 mM NaCl, 1 mM EDTA, 2 mM EGTA, 50 mM NaF, and 10 mM sodium pyrophosphate at pH 7.4) supplemented with a protease inhibitor cocktail and phosphatase inhibitor cocktail. The pellet was resuspended and rotated at 4 °C for 30 min. Next, it was centrifuged at 20,000×*g* at 4 °C for 20 min. The resulting supernatants contained the DRM fraction. The protein concentration was measured using a bicinchoninic acid (BCA) protein assay (Thermo Fisher Scientific, Waltham, MA, USA), and equal amounts of proteins from both fractions were loaded and analyzed by Western blotting.

Anti-AQP4 polyclonal antibody (A5971; Sigma–Aldrich, St. Louis, MO, USA), anti-dystroglycan antibody (ab49515l; Abcam, Cambridge, UK), anti-syntrophin antibody (1351; Millipore, Burlington, MA, USA), and anti-caveolin-1 antibody (PA1-064; ABR, Golden, CO, USA) were used as primary antibodies. Chemiluminescence detection was performed using horseradish peroxidase-conjugated secondary antibodies (Jackson Laboratory, Bar Harbor, ME, USA) and SuperSignal Substrate (Thermo Fisher Scientific), and the resulting signals were acquired with the ImageQuant LAS 4000 system (GE Healthcare, Little Chalfont, UK). Western blotting conditions were optimized to make sure the linear relationship between protein amounts and band intensities, and quantified as previously reported.[19] Band intensities were quantified using ImageJ software (National Institutes of Health [NIH], Bethesda, MD, USA).

2.4. Cell cultures

CHO cells were prepared as described previously.[21] AQP4 M1 and M23 isoforms were inserted into the pIRES-EGFP expression vector using Lipofectamine and Plus reagents (Invitrogen, Carlsbad, CA, USA) according to the manufacturer's instructions.

2.5. Data analysis

Immunoblot data were quantitatively analyzed using ImageJ software (NIH). Quantification of integrated band intensity (protein amount), bandwidth (migration pattern), and the values of individual bands were normalized to those of the control samples in the same membrane. The migration patterns of AQP4 M1 and M23 were analyzed by taking plot profiles of AQP4 from a lower to higher molecular weight. The relative position of the peak was analyzed for each band and used for statistical analyses. Calculations of DRM fraction were performed by using the band intensities of proteins of interests in each blot as well as the information regarding how much of the sample out of total amount obtained from each brain slice was used for SDS-PAGE. By dividing the former number (band intensity) by the latter (percentage of protein samples loaded on SDS-PAGE), we obtained imaginary band intensities of the proteins of interests in Non-DRM and DRM if all the protein samples collected were to be loaded and analyzed. These

values were then used to calculate the fraction of proteins in DRM in the original sample. Summary graphs show the mean ± standard error of the mean. Statistical analyses were performed using a *t*-test for two-group samples and a one-way analysis of variance (ANOVA) followed by a post-hoc Bonferroni test for samples with more than three groups. Statistically significant differences are indicated by asterisks in figures.

3. Results

To characterize the nature of AQP4 in cortical astrocytes in the brain, we first examined the detergent solubility of AQP4 using acute brain slices. Acute brain slices maintain astrocytes in physiological contexts while allowing pharmacological/pathophysiological manipulations.[19] Biochemical fractionation experiments suggested that 21% of the total AQP4 protein in the brain is localized in the 1% Triton X-100 insoluble (DRM) fraction under our experimental conditions (Supplementary Table 1 and Supplementary Fig. 1). While AQP4 is suggested to be in the macromolecular complex with syntrophin and β-dystroglycan,[22] these two proteins are more soluble to 1% Triton; thus, small populations reside in the DRM (7.3% and 1.1% for syntrophin and β-dystroglycan, respectively) (Supplementary Table 1 and Supplementary Fig. 1), suggesting a unique nature of AQP4. This result is consistent with previous studies that investigated the association between AQP4 and lipid rafts by detergent fractionation and found that β-dystroglycan is enriched in Triton-X extract and that AQP4 resides in the Triton-X insoluble fraction.[17,23]

To further investigate the molecular details of AQP4 in the non-DRM and DRM fractions, we analyzed the migration patterns of AQP4 using SDS polyacrylamide gel electrophoresis. In the non-DRM fraction, the plot profile showed two distinct peaks of bands, consistent with the presence of both the M1 (323 amino acids; predicted molecular weight of ~34 kDa) and M23 (301 amino acids; predicted molecular weight of ~32 kDa) isoforms of AQP4. In contrast, the plot profile was rather continuous in the DRM fraction with a single peak at a lower molecular weight, suggesting that this fraction is enriched in the M23 isoform with little M1 (Fig. 1).

Previous studies have shown that the expression ratio of AQP4 M1 and M23 determines the size of OAPs in the plasma membrane.[11] Stable OAPs are formed when AQP4 M23 is more highly expressed than AQP4 M1,[11] and there are multiple pools in the plasma membrane that depend on this ratio.[18] Based on the results suggesting specific enrichment of the M23 isoform of AQP4 proteins in the DRM fraction, we hypothesized that M23-dependent OAP formation makes the AQP4 proteins hardly soluble in 1% Triton. To test this hypothesis, we employed CHO cells stably expressing either the M1 or M23 isoform of AQP4 and analyzed the detergent solubility of AQP4 proteins expressed in these cells. We found striking differences between the detergent solubilities of the two isoforms of AQP4; nearly 60% of M23 proteins were insoluble in Triton, whereas less than 10% of M1 proteins were insoluble (Fig. 2A, n = 3 for each group, p = 0.0011).

Meanwhile, one study showed that AQP4 resides in the Triton-X insoluble fraction and that cholesterol depletion results in the translocation of a pool of AQP4 to the soluble fraction.[23] We thus examined whether lipid rafts are associated with the localization of AQP4 in the DRM fraction. We used caveolin-1 as a marker for lipid rafts. By depleting cholesterol, we disrupted the lipid raft and observed potential changes in both caveolin-1 and AQP4 under this condition. Interestingly, no change was identified in AQP4 in the DRM fraction even when there was a significant reduction of caveolin-1 after cholesterol depletion (Fig. 2B, n = 7 for each group, p = 0.61 for AQP4; n = 7 for control and n = 6 for MβCD, p = 0.039 for caveolin-1). These results are consistent with the idea that the insolubility of AQP4 in 1% Triton is more reliant on M23-dependent OAP formation rather than an association with lipid rafts.

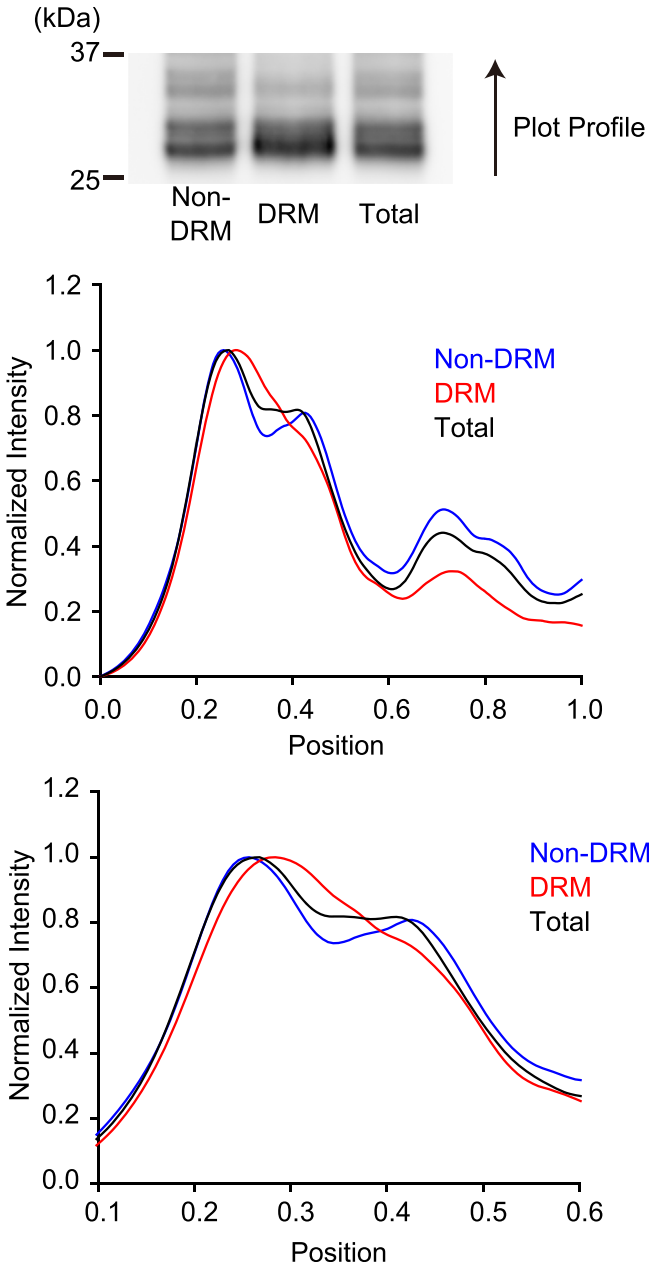

Fig. 1. AQP4 migration pattern difference in the DRM and non-DRM fractions. Representative Western blotting of AQP4 in the non-DRM and DRM fractions as well as the original lysates without fractionation (total) is shown. The intensity profiles were analyzed from the 25 to 37 kDa positions in the direction indicated by the arrow. The bottom intensity profile is the close-up view of the middle intensity profile.

Finally, we investigated whether there was any difference in the nature of AQP4 proteins in the non-DRM and DRM fractions. In particular, we focused on pathological conditions using OGD in an *in vitro* model of ischemia as described previously.[24] In brief, we incubated acute cortical brain slices with glucose-deprived ACSF that was bubbled with 95% N_2 and 5% CO_2 and compared them with those incubated with normal glucose containing ACSF bubbled with 95% O_2 and 5% CO_2. The cortical slices were subsequently used for biochemical analysis and then examined for the expression of AQP4.

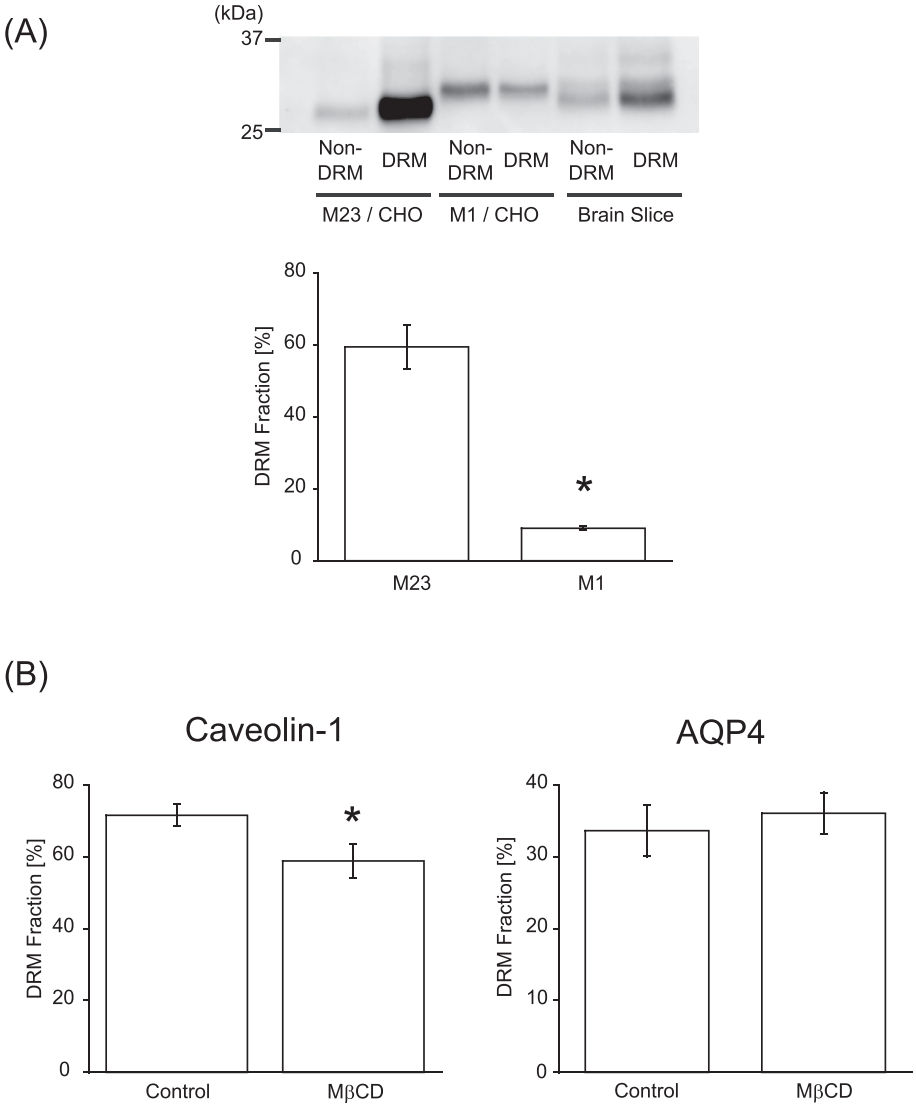

Fig. 2. Characterization of AQP4 in the DRM fraction. (A) Percentage of AQP4 M1 and M23 isoforms in the DRM fraction in CHO cells. Representative Western blotting of CHO cell lysates and brain slice lysates stained with anti-AQP4 polyclonal antibody is shown. AQP4 M23 had a higher percentage in the DRM fraction while M1 was higher in the non-DRM fraction. (B) Effect of cholesterol depletion on AQP4 in the DRM fraction. The involvement of lipid rafts was investigated in an experiment using MβCD to extract cholesterol from the membrane. The expression of caveolin-1 as a lipid raft marker significantly changed after the addition of MβCD. On the other hand, AQP4 in the DRM fraction showed no significant changes under these conditions.

The total expression level of AQP4 was significantly reduced after 60 min of OGD compared to the control before fractionation (Fig. 3, $n = 6$ for each group, $p = 0.0031$ ANOVA, $p < 0.05$ Bonferroni post-hoc mean comparison). The reduction of AQP4 at 60 min was similar to previous results of ischemia in mice[25] and consistent with the functional changes of astrocyte endfeet at this time point.[26] Although the AQP4 expression level did not change at 15 min, our previous study revealed that astrocytes respond to OGD stimulation and play important roles in neuroprotection at this time point,[24] highlighting the possibility that AQP4 may undergo molecular changes that are not reflected in its protein expression level as a whole.

Interestingly, we found that after fractionation, AQP4 in the DRM fraction had already decreased significantly after 15 min of OGD (Fig. 4, $n = 7$ for each group, $p = 0.0019$). This result suggests a unique behavior of AQP4 in the DRM fraction, revealing an earlier AQP4 response to ischemic insults.

4. Discussion

Our results showed that AQP4 in astrocytes that reside in the DRM fraction mainly consist of the AQP4 M23 isoform and appear to be in a separate pool than that of the dystrophin complex containing β−dystroglycan and syntrophin, which are thought to anchor AQP4 to the basal lamina. The insolubility of AQP4 appears to not be dependent on its association with lipid rafts but rather on its enrichment in the M23 isoform. Furthermore, AQP4 shows an early expression reduction under OGD conditions *in vitro* compared to AQP4 in the non-DRM fraction.

The finding of an AQP4 pool separated from the dystrophin complex demonstrates the possibility of differential regulation of AQP4 organization in the plasma membrane unrelated to the dystrophin complex. The association with the dystrophin complex was first postulated by Neely et al.,[27] who showed that the polarization of AQP4 is tethered by syntrophin as part of the dystrophin complex

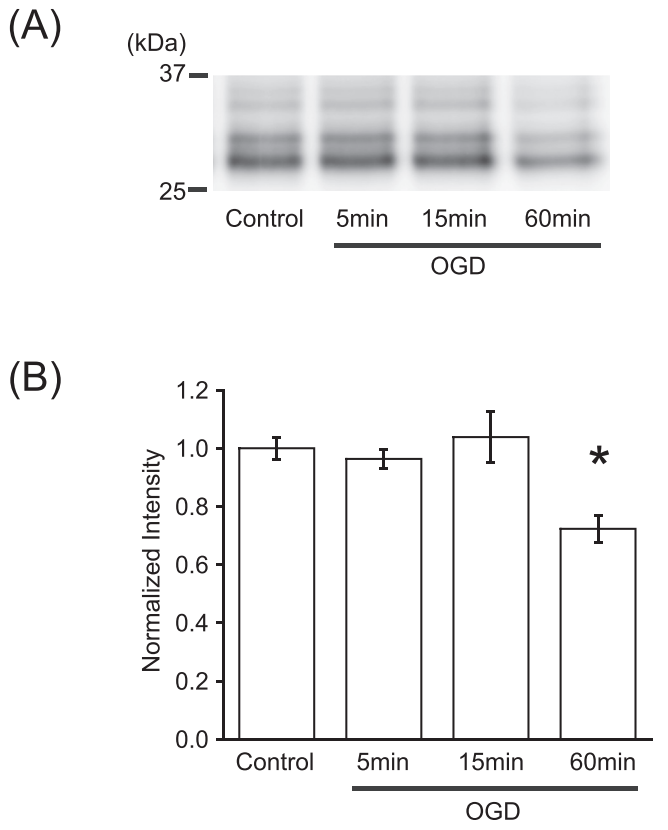

Fig. 3. Time course of the total expression of AQP4 under OGD conditions. (A) Representative Western blotting of brain slice lysates stained with anti-AQP4 polyclonal antibody under OGD conditions. (B) Quantification of the data. There were no significant changes in AQP4 protein expression after 5 min and 15 min, but it was reduced at 60 min.

using syntrophin knockout mice. A later study by Nicchia et al.[18] identified several pools of AQP4, some of which were not co-purified with β-dystroglycan and dystrophin. They concluded that there may be a different mechanism involving this other pool under pathological conditions independent of the dystrophin complex.[18] This idea is also supported by the finding that AQP4 is separated from β-dystroglycan after fractionation into the DRM and non-DRM fractions.[17]

An alternative hypothesis regarding the regulation of this distinct pool of AQP4 involves lipid rafts. Lipid rafts have been defined empirically based on their low density and insolubility in 1% Triton X-100. They function in membrane trafficking, signal transduction, and depolarization. The DRM involves the artificial coalescence of raft constituents into an insoluble residue by a process that is not fully understood. It has been observed that there are changes in the DRM association upon induction of physiologically relevant stimuli.[16,28] We found that cholesterol extraction does not result in an AQP4 change in the DRM fraction even though it significantly changes caveolin-1, which is known to reside in the DRM. Discrepancy of results of ours and previous study[17] may reflect a different biochemical nature of AQP4 in cell culture system compared to those in brain tissues. In this regard, while acute brain slice system is suitable for pharmacological and pathophysiological analyses of the brain tissues,[19] cares need to be taken in extrapolating the current results to *in vivo* situation, especially under complex pathophysiology of ischemia.

It is conceivable that AQP4 in the DRM fraction is associated with a larger size due to the dominance of the M23 isoform. AQP4 has two classical isoforms, M1 and M23, and two different translation initiation sites in the same gene, AQP4 M1 at Met-1 and AQP4 M23 at Met-23. The size of AQP4 aggregation in the plasma membrane is considered to be larger when it consists of more AQP4 M23.[11,14] In order to evaluate the difference between AQP4 M1 and M23 in the DRM and non-DRM fractions, we used plot profiles to

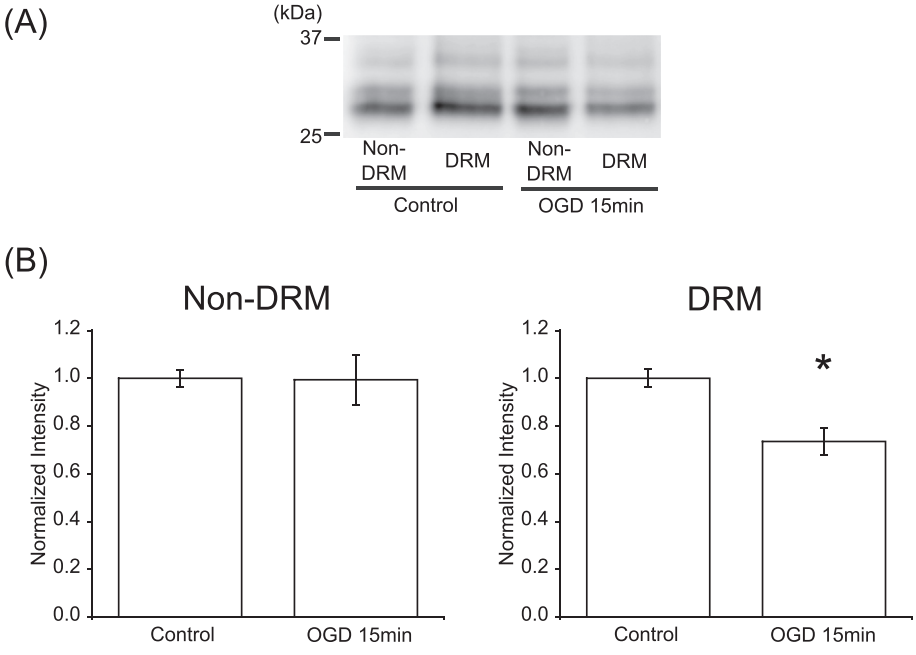

Fig. 4. AQP4 expression changes under OGD conditions after protein fractionation. (A) Representative Western blotting of AQP4 proteins in the non-DRM and DRM fractions at 15 min under control or OGD conditions. (B) Quantification of the results. After protein fractionation, AQP4 expression was significantly reduced in the DRM fraction compared to the control after 15 min of OGD. In contrast, AQP4 in the non-DRM fraction did not change significantly.

analyze the two isoforms in both fractions. We found that the DRM fraction is enriched with the M23 isoform and consists of minimal M1, supporting our hypothesis that the insolubility of AQP4 in the DRM fraction is more likely caused by the size of the OAPs in the DRM fraction. This result is further supported by the observation that CHO cells expressing only the M23 isoform reside mostly in the DRM fraction compared to CHO cells expressing only the M1 isoform (Fig. 2A). The conformation of AQP4 related to the ratio of M1 and M23 isoforms has been illustrated in several studies. Furman et al.[11] observed the assembly of AQP4 using electron microscopy in the membrane of CHO cells that express AQP4 M1, M23, or both. A larger island of AQP4 was observed in cells transfected with only M23, and the sizes varied when cells were transfected with both isoform.[11] A mathematical model that analyzes the role of M1/M23 composition in OAP assembly predicted that OAP size increases with an increasing M23:M1 ratio and preferential localization of M1 AQP4 at the periphery of OAPs.[29] It should also be noted that existence of AQP4 isoforms other than M1 and M23 have been suggested.[30,31] For example, a recent finding of the extended AQP4 isoform generated by translational readthrough, AQP4ex, shed light into the supramolecular organization of AQP4. Palazzo et al.[31] showed that in the absence of AQP4ex, the organization of OAP in the perivascular changes. This mechanism supports the idea that OAPs rearrange their sizes and undergo reorganization in certain condition. Finally, various post-translational modification including phosphorylations are known for AQP4, which may explain different degrees of bandwidth observed for M1/M23 and Non-DRM/DRM in our study. Therefore, while our data can be explained by the two major isoforms of M1 and M23, further studies may illuminate more complex combinatorial effects of various isoforms and post-translational modifications to determine the biochemical properties of AQP4 in the brain. Regardless of detailed mechanisms, these various factors may affect AQP4 functions at the plasma membrane and/or through dynamic regulation of subcellular localization via endocytosis/exocytosis.

The biological importance of OAP formation is not fully understood. It has shown a role in astrocyte migration function,[32] epilepsy,[33] traumatic brain injury,[34] brain edema,[8] glioma[12] as well as normal protein expressions.[35] Loss of perivascular AQP4 polarization is a key feature in pathological conditions in astrocytes. Here, we showed that AQP4 in the DRM fraction was reduced early under OGD conditions compared to the non-DRM fraction (Fig. 4), leading to changes in the DRM enrichment of AQP4 proteins in the brain. On the contrary, the total expression of AQP4 did not change at the same time point (Fig. 3), likely because the DRM fraction only constitutes 20% of all AQP4 proteins. This result suggests the occurrence of another process in the DRM fraction at 15 min after OGD that is not reflected in the total AQP4 expression. Here, it should be noted that our detailed analyses revealed that OGD induced global changes in the expressions and distributions of proteins under our experimental condition, including β-actin and α-tubulin that we have routinely used for internal controls in western blotting analyses. As such, to avoid drawing erroneous conclusions by subjective choice of particular protein as a loading control, OGD analyses were performed by normalizing total protein amounts. AQP4 OAPs have been shown to be disrupted after 90 min of middle cerebral artery occlusion in mice.[25] The reduction of AQP4 expression under ischemia is thought to be a mechanism to reduce cytotoxic edema. It was also shown that AQP4 knockout mice have a lower hemispheric enlargement and better survival rate than AQP4 wild-type mice.[8] Thus, it is tempting to suggest that the reduction of AQP4 is a result of the disruption of OAPs after ischemia, which is a mechanism for reducing brain edema.

In summary, AQP4 in the DRM fraction consists largely of the M23 isoform. Its solubility is contingent upon on the large array that depends on the ratio of M1 and M23, and it is not dependent on lipid raft regulation. This fraction reduced earlier than the total expression of AQP4 under OGD conditions, which may be related to the role of this channel in limiting cerebral edema after ischemia.

Declaration of competing interest

The authors indicated no potential conflicts of interest.

Acknowledgements

This work was supported by JSPS KAKENHI (grant nos. 16K07065, 20H02881 and 20K20593). We would like to thank Y. Abe (Keio University) for providing us with the CHO cell lines that stably express AQP4.

Appendix A. Supplementary data

Supplementary data to this article can be found online at https://doi.org/10.1016/j.jphs.2021.03.003.

References

1. Ishibashi K. New members of mammalian aquaporins: AQP10–AQP12. In: Beitz E, ed. *Aquaporins*., vol. 190. Springer Berlin Heidelberg; 2009:251–262 https://doi.org/10.1007/978-3-540-79885-9_13.
2. Verkman AS. Aquaporins at a glance. *J Cell Sci*. 2011;124(13):2107–2112. https://doi.org/10.1242/jcs.079467.
3. Assentoft M, Larsen BR, MacAulay N. Regulation and function of AQP4 in the central nervous system. *Neurochem Res*. 2015;40(12):2615–2627. https://doi.org/10.1007/s11064-015-1519-z.
4. Nagelhus EA, Ottersen OP. Physiological roles of aquaporin-4 in brain. *Physiol Rev*. 2013;93(4):1543–1562. https://doi.org/10.1152/physrev.00011.2013.
5. Hu H, Yao H, Zhang W, et al. Increased expression of aquaporin-4 in human traumatic brain injury and brain tumors. *J Zhejiang Univ - Sci*. 2005;6B(1):33–37. https://doi.org/10.1631/jzus.2005.B0033.
6. Vella J. The central role of aquaporins in the pathophysiology of ischemic stroke. *Front Cell Neurosci*. 2015;9. https://doi.org/10.3389/fncel.2015.00108.
7. Maugeri R, Schiera G, Di Liegro C, Fricano A, Iacopino D, Di Liegro I. Aquaporins and brain tumors. *Int J Mol Sci*. 2016;17(7):1029. https://doi.org/10.3390/ijms17071029.
8. Manley GT, Fujimura M, Ma T, et al. Aquaporin-4 deletion in mice reduces brain edema after acute water intoxication and ischemic stroke. *Nat Med*. 2000;6(2):159–163. https://doi.org/10.1038/72256.
9. Hinson SR, Pittock SJ, Lucchinetti CF, et al. Pathogenic potential of IgG binding to water channel extracellular domain in neuromyelitis optica. *Neurology*. 2007;69(24):2221–2231. https://doi.org/10.1212/01.WNL.0000289761.64862.ce.
10. Lu M, Lee MD, Smith BL, et al. The human AQP4 gene: definition of the locus encoding two water channel polypeptides in brain. *Proc Natl Acad Sci Unit States Am*. 1996;93(20):10908–10912. https://doi.org/10.1073/pnas.93.20.10908.
11. Furman CS, Gorelick-Feldman DA, Davidson KGV, et al. Aquaporin-4 square array assembly: opposing actions of M1 and M23 isoforms. *Proc Natl Acad Sci Unit States Am*. 2003;100(23):13609–13614. https://doi.org/10.1073/pnas.2235843100.
12. Simone L, Pisani F, Mola MG, et al. AQP4 aggregation state is a determinant for glioma cell fate. *Canc Res*. 2019;79(9):2182–2194. https://doi.org/10.1158/0008-5472.CAN-18-2015.
13. Hinson SR, Romero MF, Popescu BFG, et al. Molecular outcomes of neuromyelitis optica (NMO)-IgG binding to aquaporin-4 in astrocytes. *Proc Natl Acad Sci Unit States Am*. 2011;109:1245–1250. https://doi.org/10.1073/pnas.1109980108.
14. Crane JM, Bennett JL, Verkman AS. Live cell analysis of aquaporin-4 M1/M23 interactions and regulated orthogonal array assembly in glial cells. *J Biol Chem*. 2009;284(51):35850–35860. https://doi.org/10.1074/jbc.M109.071670.
15. Sun Y, Zhang Y-L, Hu S-G, Li X-Q, Tang C-H. Isolation and characterization of detergent-resistant membranes from rat spermatozoa. *Asian J Androl*. 2014;16(5):790. https://doi.org/10.4103/1008-682X.132979.
16. Lingwood D, Kaiser H-J, Levental I, Simons K. Lipid rafts as functional heterogeneity in cell membranes. *Biochem Soc Trans*. 2009;37(5):955–960. https://doi.org/10.1042/BST0370955.
17. Noël G, Tham DKL, Moukhles H. Interdependence of laminin-mediated clustering of lipid rafts and the dystrophin complex in astrocytes. *J Biol Chem*. 2009;284(29):19694–19704. https://doi.org/10.1074/jbc.M109.010090.
18. Nicchia GP, Cogotzi L, Rossi A, et al. Expression of multiple AQP4 pools in the plasma membrane and their association with the dystrophin complex:

aquaporin-4 organization in the plasma membrane. *J Neurochem*. 2008;105(6):2156–2165. https://doi.org/10.1111/j.1471-4159.2008.05302.x.
19. Gondo A, Shinotsuka T, Morita A, Abe Y, Yasui M, Nuriya M. Sustained down-regulation of β-dystroglycan and associated dysfunctions of astrocytic end-feet in epileptic cerebral cortex. *J Biol Chem*. 2014;289(44):30279–30288. https://doi.org/10.1074/jbc.M114.588384.
20. Hering H, Lin C-C, Sheng M. Lipid rafts in the maintenance of synapses, dendritic spines, and surface AMPA receptor stability. *J Neurosci*. 2003;23(8):3262–3271. https://doi.org/10.1523/JNEUROSCI.23-08-03262.2003.
21. Miyazaki K, Abe Y, Iwanari H, et al. Establishment of monoclonal antibodies against the extracellular domain that block binding of NMO-IgG to AQP4. *J Neuroimmunol*. 2013;260(1–2):107–116. https://doi.org/10.1016/j.jneuroim.2013.03.003.
22. Amiry-Moghaddam M, Frydenlund DS, Ottersen OP. Anchoring of aquaporin-4 in brain: molecular mechanisms and implications for the physiology and pathophysiology of water transport. *Neuroscience*. 2004;129(4):997–1008. https://doi.org/10.1016/j.neuroscience.2004.08.049.
23. Asakura K, Ueda A, Shima S, et al. Targeting of aquaporin 4 into lipid rafts and its biological significance. *Brain Res*. 2014;1583:237–244. https://doi.org/10.1016/j.brainres.2014.08.014.
24. Shinotsuka T, Yasui M, Nuriya M. Astrocytic gap junctional networks suppress cellular damage in an in vitro model of ischemia. *Biochem Biophys Res Commun*. 2014;444:171–176. https://doi.org/10.1016/j.bbrc.2014.01.035.
25. Frydenlund DS, Bhardwaj A, Otsuka T, et al. Temporary loss of perivascular aquaporin-4 in neocortex after transient middle cerebral artery occlusion in mice. *Proc Natl Acad Sci Unit States Am*. 2006;103(36):13532–13536. https://doi.org/10.1073/pnas.0605796103.
26. Nuriya M, Shinotsuka T, Yasui M. Diffusion properties of molecules at the blood-brain interface: potential contributions of astrocyte endfeet to diffusion barrier functions. *Cerebr Cortex*. 2013;23(9):2118–2126. https://doi.org/10.1093/cercor/bhs198.
27. Neely JD, Amiry-Moghaddam M, Ottersen OP, Froehner SC, Agre P, Adams ME. Syntrophin-dependent expression and localization of Aquaporin-4 water channel protein. *Proc Natl Acad Sci Unit States Am*. 2001;98(24):14108–14113. https://doi.org/10.1073/pnas.241508198.
28. Pike LJ. Lipid rafts: bringing order to chaos. *J Lipid Res*. 2003;44(4):655–667. https://doi.org/10.1194/jlr.R200021-JLR200.
29. Jin B-J, Rossi A, Verkman AS. Model of aquaporin-4 supramolecular assembly in orthogonal arrays based on heterotetrameric association of M1-M23 isoforms. *Biophys J*. 2011;100(12):2936–2945. https://doi.org/10.1016/j.bpj.2011.05.012.
30. De Bellis M, Pisani F, Mola MG, et al. Translational readthrough generates new astrocyte AQP4 isoforms that modulate supramolecular clustering, glial end-feet localization, and water transport: DE BELLIS et al. *Glia*. 2017;65(5):790–803. https://doi.org/10.1002/glia.23126.
31. Palazzo C, Buccoliero C, Mola MG, et al. AQP4ex is crucial for the anchoring of AQP4 at the astrocyte end-feet and for neuromyelitis optica antibody binding. *Acta Neuropathol Commun*. 2019;7(1):51. https://doi.org/10.1186/s40478-019-0707-5.
32. Smith AJ, Jin B-J, Ratelade J, Verkman AS. Aggregation state determines the localization and function of M1– and M23–aquaporin-4 in astrocytes. *J Cell Biol*. 2014;204(4):559–573. https://doi.org/10.1083/jcb.201308118.
33. Binder DK, Yao X, Zador Z, Sick TJ, Verkman AS, Manley GT. Increased seizure duration and slowed potassium kinetics in mice lacking aquaporin-4 water channels. *Glia*. 2006;53:631–636. https://doi.org/10.1002/glia.20318.
34. Iliff JJ, Chen MJ, Plog BA, et al. Impairment of glymphatic pathway function promotes tau pathology after traumatic brain injury. *J Neurosci*. 2014;34(49):16180–16193. https://doi.org/10.1523/JNEUROSCI.3020-14.2014.
35. de Bellis M, Cibelli A, Mola MG, et al. Orthogonal arrays of particle assembly are essential for normal aquaporin-4 expression level in the brain. *Glia*. Published online September 18, 2020:glia.23909. doi:10.1002/glia.23909.